Available online at www.sciencedirect.com

ScienceDirect

Procedia Engineering 2 (2010) 815–824

Procedia Engineering

www.elsevier.com/locate/procedia

Fatigue 2010

On thermo-mechanical fatigue in single crystal Ni-base superalloys

Robert L. Amaro[a], Stephen D. Antolovich[b]*, Richard W. Neu[a,b], Alexander Staroselsky[c]

[a] *Woodruff School of Mechanical Engineering and Mechanical Properties Research Laboratory, Georgia Institute of Technology, Atlanta GA, 30332, USA*

[b] *School of Materials Science and Engineering and Mechanical Properties Research Laboratory, Georgia Institute of Technology, Atlanta GA, 30332, USA*

[c] *Pratt & Whitney, 400 Main St. East Hartford CT, 06108, USA*

Received 28 February 2010; revised 10 March 2010; accepted 15 March 2010

Abstract

Thermo-mechanical fatigue (TMF) is a critical damage process in gas turbine jet engines. Reliable life prediction methodologies are required both for design and life management. Current life estimation approaches are computationally burdensome and/or semi-empirical, significantly limiting their application. Complexity comes about from the multiplicity of damage processes which occur during the simultaneously changing temperatures and loads, characteristic of TMF. Furthermore, these processes interact in ways that are not observed for isothermal LCF. These interactions usually accelerate damage processes and result in significantly reduced TMF life, when compared to other fatigue scenarios. The results of a multiphased approach to life prediction will be presented. In phase I the Neu-Sehitoglu (N-S) cumulative damage model was used to: a) provide initial life predictions and b) identify processes and interactions which most significantly control the life under TMF loading. The N-S model is based on a linear damage summation rule which both explicitly and implicitly includes damage interactions. In phase II a sensitivity analysis incorporating statistical concepts was performed on the N-S model parameters. Specifically a nonlinear optimization was performed to determine optimal parameter values in order to maximize agreement with experimental results (well within 2X). In phase III, informed by phases I and II, a physics-based fatigue/oxidation (also recognizing creep effects) model was developed which correctly predicts effects of frequency, hold-time, temperature, and strain range and oxidation kinetics.

Keywords: Thermo-mechanical fatigue; TMF; high temperature; life modelling; fatigue life; fatigue life prediction; damage mechanisms

1. Introduction

Superalloys are a class of metals that exhibit superior high temperature properties such as very high strength at temperatures up to 85% of their melting points [1] and were developed for use in aero and power generation turbines. Of the different forms in which superalloys are manufactured, single crystal superalloys (SXSA) are favored for use as blade materials in the hot section of turbines because of their fortuitous primary crystal orientation and resulting radial modulus, as well as their superior creep properties resulting from the elimination of grain

* Corresponding author. Tel.: +0-404-894-2879; fax: +0-404-894-9140.
E-mail address: stevea@gatech.edu.

1877-7058
doi:10.1016/j.proeng.2010.03.088

boundaries. The use of single crystal superalloys in the hot section of turbines has enabled higher turbine temperatures, thereby increasing efficiency and decreasing pollution [2]. In addition to high temperatures, turbine blades experience relatively high strains induced by centrifugal forces coupled with thermal and mechanical strain transients brought on by stress concentrations, vibrational mis-tuning, start-up and shut-down cycling as well as changing load demands. This type of loading, (i.e. temperature and mechanical strains varying simultaneously in a cyclic manner) is called thermo-mechanical fatigue (TMF). In order to design a component to withstand TMF, the material deformation response to each of the independent conditions with respect to the material's anisotropy, as well as the interaction between the independent damage modes must be understood. Competing damage mechanisms for out-of-phase (OP) TMF primarily include environmental and fatigue, while creep and fatigue dominate in in-phase (IP) TMF. Current TMF life predictive schemes include damage summation in a Miner's rule fashion, critical plane theories [3, 4], micromechanics based equivalent inclusion methods based upon Eshelby solutions [5] and cumulative damage models [6-8], among others. While these models do an acceptable job of life prediction in some situations, they do not adequately account for inherent damage mechanism interaction and therefore do not provide the level of understanding required for in-depth component analysis and reliable life prediction. Damage mechanisms inherent to TMF conditions can interact constructively or destructively, depending upon the boundary conditions and mechanisms present. As such, a physics-based life prediction model would be a powerful tool when designing new components or next-generation materials. The ultimate goal of this work is to propose such a model. First, however, developing a deeper understanding of dominant damage mechanisms, as well as their interactions, is paramount. To address this issue a cumulative damage model is employed which facilitates the identification of the dominant damage mechanisms present for the experimental results studied.

2. Phase I: Life estimation using Neu-Sehitoglu model

In this phase of the research study the cumulative damage life model of Neu and Sehitoglu (N-S) [6] was used to predict OP TMF lives of previously tested single crystal PWA 1484. This model has been successfully used to predict TMF lives for the superalloys Mar-M247 and GTD-111 [7, 9]. The N-S cumulative damage model has the general form,

$$N_i = \left(\frac{1}{N_i^{fat}} + \frac{1}{N_i^{cr}} + \frac{1}{N_i^{env}} \right)^{-1} \tag{1}$$

where the fatigue, creep and environmental modules, modified for directionally solidified materials [10], are defined respectively as

$$N_i^{fat} = C_{in} f_{in}(\omega) \left(\Delta\varepsilon_{mech}\right)^{d_{in}} \tag{2}$$

$$N_i^{cr} = \Theta_{CR}^{TMF} \exp\left(\frac{-B' f_{CR}\left(\sigma_{tens}\right)^{-k}}{RT} \right) \Phi^{CREEP} \tag{3}$$

$$\frac{1}{N_i^{env}} = \left[\frac{h_{cr}\delta_0}{B\Phi^{ENV}\left(K_{peff}^{ENV} + K_{peff}^{\gamma'}\right)} \right]^{-1/\beta} \frac{2\left(\Delta\varepsilon_{mech}\right)^{\left(2/\beta\right)+1}}{\dot{\varepsilon}^{1-\alpha/\beta}} \tag{4}$$

The fatigue module includes a orientation dependent term, ($f_{in}(\omega)$), a pre-factor and exponential. The orientation term accounts for directionally solidified or single crystal material orientation with respect to loading, and the pre-factor and exponential terms are both fit to lower-temperature low cycle fatigue (LCF) data to minimize

environmental and creep effects. The creep module was not used in this study as OP TMF lives were being estimated. The environmental-fatigue module also includes a phasing term,

$$\Phi^{ENV} = \frac{1}{t_c}\int_0^{t_c} \phi^{ENV}\, dt \tag{8}$$

where ϕ^{ENV} is defined as

$$\phi^{ENV} = \exp\left[-\frac{1}{2}\left(\frac{\left(\dot{\varepsilon}_{th}/\dot{\varepsilon}_{mech}\right)+1}{\xi^{OX}}\right)^2\right] \tag{9}$$

in which ζ^{ox} accounts for the sensitivity of oxidation damage to cyclic phasing. The phasing term, Φ^{ENV}, effectively accounts for temperature-strain phase differences by forcing the term to a value of one for OP TMF and zero for IP TMF. The oxidation and γ' depletion terms within the environmental-fatigue module, K^{ENV} and $K^{\gamma'}$ respectively, are defined as,

$$K_{peff}^{ENV} = \frac{1}{t_c}\int_0^{t_c} D_{OX}\exp\left(\frac{-Q_{OX}}{R\cdot T(t)}\right)dt \tag{10}$$

and

$$K_{peff}^{\gamma'} = \frac{1}{t_c}\int_0^{t_c} D_{\gamma'}\exp\left(\frac{-Q_{\gamma'}}{R\cdot T(t)}\right)dt \tag{11}$$

The terms Dox and Qox are the oxidation diffusion coefficient and activation energies, while the $D_{\gamma'}$ and $Q_{\gamma'}$ are the γ' diffusion coefficient and activation energies, respectively. The environmental-fatigue module also includes terms which account for: 1) the material ductility within the environmentally affected zone, δo, 2) the critical crack length at which the environmental attack trails behind the advancing crack tip, hcr 3) the strain rate sensitivity, α; and 4) terms accounting for total environmentally induced crack length, B and β. These equations effectively account for the independent damage mechanisms of fatigue, creep and environment-fatigue when used to estimate thermo-mechanical fatigue (TMF) component life. The interested reader is directed to references [6, 9, 10] for an in-depth discussion of each term used in the N-S model.

In this study the Neu-Sehitoglu model is used to predict TMF lives for the single crystal PWA 1484 test data provided in Table 1. The table lists each tests waveform, maximum and minimum temperatures; mechanical strain range; R_ε, defined as $\varepsilon_{min}/\varepsilon_{max}$; and number of cycles to crack initiation. These tests were performed in the Mechanical Properties Research Laboratory at Georgia Institute of Technology. Table 1 divides the tests results into three sections: 1) the top section provides results for base-line TMF tests, 2) the middle section provides results for TMF tests having varied testing parameters and 3) the lower section of Table 1 provides test results for bithermal fatigue (BiF) tests. Out-of-phase BiF tests are strain-controlled fatigue tests in which a single cycle consists of an isothermal compressive half-cycle occurring at the maximum temperature, followed by stress-free temperature change to the minimum temperature and finally a tensile half-cycle which occurs isothermally at the minimum temperature, followed by stress-free temperature change to the maximum temperature. The purpose of the first and second phase of this research is to determine dominant damage mechanisms in OP TMF tests, and as such only the results provided in the first and second section of Table 1 are used for N-S model studies.

To determine constants in the N-S model, the fatigue module was fit using PWA 1480 LCF lives [11] due to lack of PWA 1484 LCF data. The environmental-fatigue module constants used in this study were previously fit using the superalloy MAR-M247 by Sehitoglu and Boismier [7] and are shown in Table 2 along with the calculated fatigue module constants.

Table 1. PWA 1484 TMF and BiF test data

Wave form	Min Temp (deg C)	Max Temp (deg C)	Δε(mech) (%)	R_ε (-)	Ni (cycle)
OP-TMF	550	1050	1.3	-0.95	107
OP-TMF	550	1050	0.9	-0.91	471
OP-TMF	550	1050	0.5	-0.82	3738
OP-TMF	550	1050	1.3	-0.39	89
OP-TMF	550	1050	1.3	-0.96	461
OP-TMF	550	1050	0.5	-1.00	1810
OP-TMF	550	1050	0.9	-0.95	610
OP-TMF*	550	1050	1.3	-0.59	64
OP-BiF	550	1050	1.3	-0.80	76
OP-BiF	550	1050	0.9	-0.93	370
OP-BiF	550	1050	0.7	-1.00	421

* 300s high-temp hold

Table 2. Environmental fatigue and fatigue module constants

Term	Value	Units	Term	Value	Units	Term	Value	Units
α	0.75	-	δ	1.12E-10	$\mu m*s^{(-0.75)}$	$D_{\gamma'}$	8570.00	μm^2*s
β	1.5	-	D_{ox}	15400.00	μm^2*s	$Q_{\gamma'}$	163.30	kJ/mol
B	0.00693	$s^{(-.5)}$	Q_{ox}	175.90	kJ/mol	C_{in}	1.63E-07	-
ζ	0.44	-	h_{cr}	461.40	μm	d_{in}	-5.4306	-

Life estimation determined by the environmental-fatigue module only, using the constants provided in Table 2, is shown in Fig 1-a., while the overall Neu-Sehitoglu life estimation is shown in Fig 1-b. One can see from Figure 1 that the environmental fatigue module has primary influence on overall life predictive trends in the N-S model, as can be seen by comparing the slopes of the trend lines in Fig 1.

The use of model constants fit to materials other than PWA 1484 was done purely out of necessity. The results, however, indicate that the model may be somewhat insensitive to the material from which the constants are derived, as long as all materials in question are of the same class, nickel-base superalloys in this case. This assertion is supported by the slope of the life estimation relationships and will be validated in Phase II of this work where a sensitivity analysis is performed.

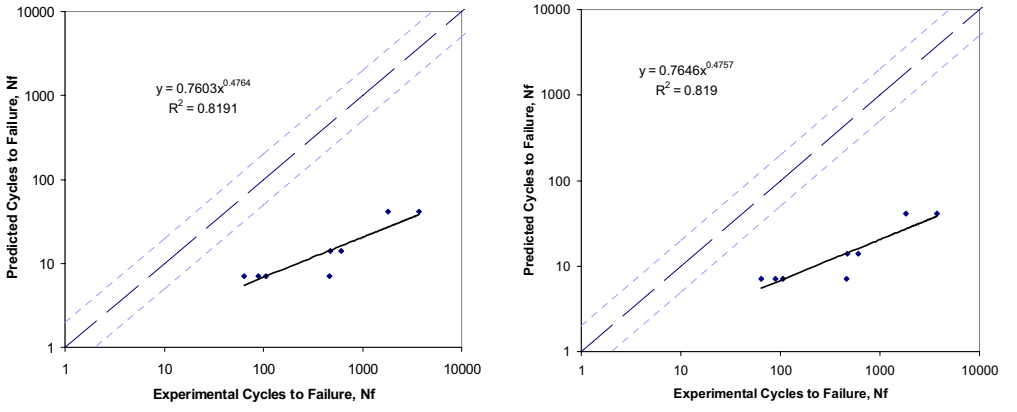

Fig. 1. (a) Life estimation using environmental-fatigue module- all TMF data (b)life estimation using Neu-Sehitoglu cumulative damage model – all TMF data; Both using constants from Table 2

Phase I of this study has shown that the environmental-fatigue module is primarily responsible for life estimation when using the N-S cumulative damage model to estimate OP TMF lives. This result is expected given the load-temperature interactions occurring during the OP cycle. Phase II of this study will determine which components of this module affect life estimation most, as well as estimating optimum values for these parameters.

3. Phase II: Neu-Sehitoglu parameter sensitivity analysis

The primary results from phase I indicate that an environmental-fatigue term dominates life prediction in the N-S model as applied to OP TMF. Additionally, results indicate that it may not be necessary to calibrate all of the model parameters for each particular material of interest. Phase II of this work explore these hypotheses.

In order to determine the sensitivity of the Neu-Sehitoglu life estimation results to the various input parameters, a study was performed in which each parameter was varied by a specified amount while holding all other inputs at nominal values. Each input was varied by a minimum of +/- 20% in 0.5% increments. The input parameters which were studied as well as their nominal values are shown in Table 2. Though the sensitivities of all parameters utilized in the environmental-fatigue module were studied, four parameters had the highest impact on life estimation: they are the activation energies (Q_{ox} and $Q_{\gamma'}$) used in the oxidation, γ' depletion terms (K^{ENV} and $K^{\gamma'}$), as well as the terms α and β. The percent change of each of these influential environmental-fatigue term's parameters versus percent change in total estimated life is shown in Figures 3 and 4. Figure 3-b, for example, indicates that there is a 4:1 relationship between the overall life prediction results and the $Q_{\gamma'}$ value, when starting from the baseline values. Overall, variation in the strain exponent, α, has the most influence on life prediction, followed by the exponent β, γ' activation energy, $Q_{\gamma'}$, and the oxidation activation energy, Q_{ox}. Since these four parameters have the greatest effect upon life estimation sensitivity it is assumed that they are material specific. Rather than perform lengthy tests to determine the material-specific values for these four parameters, a variation of parameters analysis was performed in order to determine a best engineering fit. If successful, a minimal number of tests would be required to calibrate and implement the N-S cumulative damage model. The variation of parameters was implemented using an error minimization algorithm in MATLAB. The algorithm first estimates the TMF lives for the tests presented in Table 1 using the N-S model, it then compares the life estimation to the actual life, and finally the algorithm varies the input parameters before repeating the process. The algorithm searches for optimal parameter values until the differences in the predicted and measured lives were minimized. The minimization algorithm was used to determine the values of all four of the most influential parameters while calibrating the model to the baseline TMF results provided at the top of Table 1. The resulting parameter values are shown in Table 3. Calibration results from the variation of parameters study varying $Q_{\gamma'}$, Q_{ox}, α and β are shown in Fig 5-a. Life estimation results for all TMF data, using calibrated constants in Table 3, is shown in Fig 5-b.

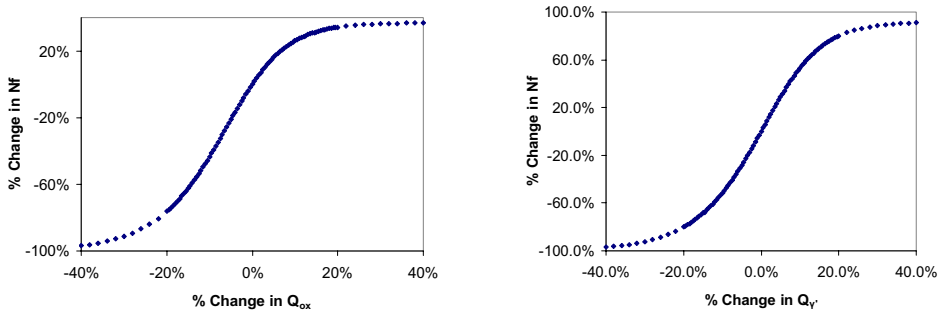

Fig. 3. (a) %-change of N_f vs. %-change of Q_{ox}; (b) %-change of N_f vs. %-change of $Q_{\gamma'}$

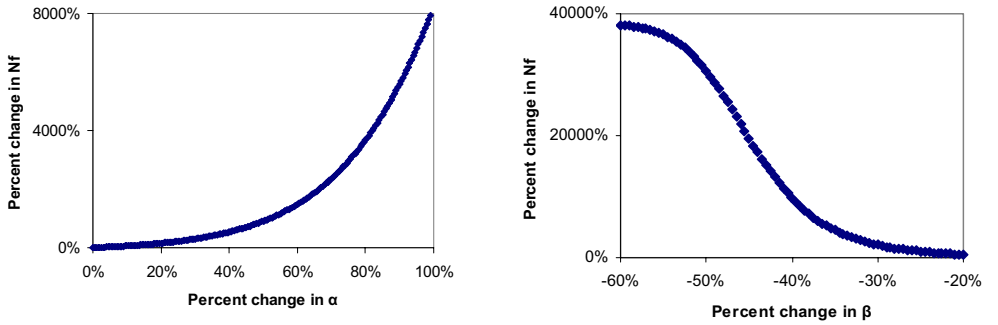

Fig. 4. (a) %-change of N_f vs. %-change of α; (b) %-change of N_f vs. %-change of β

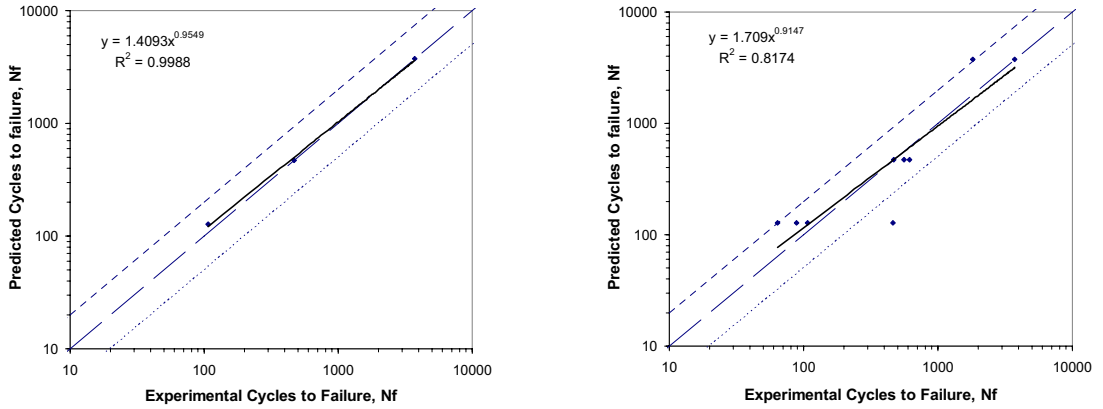

Fig. 5. (a) Calibration of N-S model using base-line TMF tests, variation of 4 parameters: $Q_{\gamma'}$, Q_{ox}, α and β; (b) Life estimation of TMF tests, variation of 4 parameters: $Q_{\gamma'}$, and Q_{ox}, α and β

Table 3. Results of variation of parameters study- calibration using baseline TMF data

Parameter	Value
$Q_{\gamma'}$	88.4 kJ/mol
Q_{ox}	99.8 kJ/mol
α	1.50
β	1.00

One can compare the calibrated parameter values in Table 3 to the baseline values in Table2. Using the knowledge gained from Phase I of this work, the influential environmental-fatigue parameters as well as their optimal values were determined in Phase II. The result is a computationally inexpensive life estimation framework requiring minimal up-front tests to calibrate. Results of Phase II, shown in Fig 5-b and Table 3, support the efficacy of the N-S model to make excellent engineering predictions.

4. Phase III: Physics-Based Fatigue-Oxidation Model

The analysis in Phases I and II of this research provided insight to Phase III in several ways. 1) OP TMF life trends are dominated by environmental-fatigue interactions, as indicated in Figure 1. 2) The dominant factors

affecting environmental-fatigue interactions are the mass transport diffusion activation energies (Q_{ox} and $Q_{\gamma'}$) as well as effects of applied strain (α and β in the N-S model). To address these points, a physics-based fatigue/oxidation life estimation model is proposed which accounts for fatigue, environment, crystal orientation and microstructural evolution.

Suppose that there exists a region of compromised base material near the edge of a single crystal experiencing uniaxial fatigue. The compromised material may result from an oxide spike, a γ' depleted zone, or an interdendritic region. If persistent slip bands, caused by fatigue, impinge on this region, a crack will initiate. This situation is shown in Figure 6.

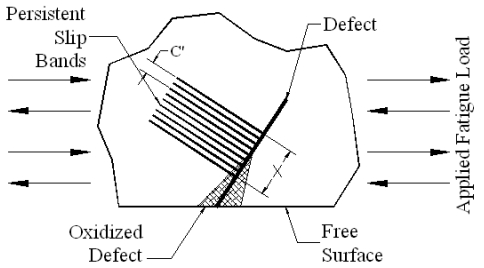

Fig. 6. Geometry in which persistent slip bands impinge upon an oxide spike

One can quantify the effects that the slip bands' interaction has upon the degraded base material via the hypothesis that a critical crack length X_{crit}, exists when a minimum number of slip bands intersect the defect,

$$X_{crit} = N_s C' \tag{12}$$

where N_s is the number of slip bands intersecting the degraded base material and C' is the average persistent slip band spacing. The general equation for slip band spacing was first proposed by Diedrich et al. [12]

$$C' = A\Delta\varepsilon_{in}^{-S} \tag{13}$$

The oxide kinetics, related to the critical crack length, are governed by

$$X = \left[D_o \exp\left(\frac{-Q'}{R \cdot T_{eff}} \right) t \right]^n \tag{14}$$

Where D_0 is the oxidation diffusion coefficient, Q' is the effective activation energy, R the universal gas constant, T_{eff} the effective temperature, t the time at the effective temperature and n an exponent fit to experimental results. The effective temperature term is defined by [13]

$$\exp\left(\frac{-Q'}{R \cdot T_{eff}} \right) = \frac{1}{t_c} \int_0^{t_c} \exp\left(\frac{-Q'}{R \cdot T(t)} \right) dt \tag{15}$$

where t_c is the cycle time and T(t) is the cycle temperature as a function of time. A crack of critical length will develop when a sufficient number of slip bands impinges upon the compromised base material, as indicated in equation 12. Combining equations 13 and 14 into equation 12 gives:

$$N_i = \frac{N_s A}{D_0^n} \left(\frac{1}{\Delta\varepsilon_{in}} \right)^s \left[\exp\left(\frac{Q'}{R \cdot T_{eff}} \right) \frac{\nu}{\nu \cdot t_h + 1/2} \right]^n \tag{16}$$

where ν is the cycle frequency, t_h is the time of a high-temperature hold event within the cycle. Equation 16, first presented in a modified form by McDowell et al. in 1991 [13], provides a life estimation scheme that accounts for fatigue and environmental interactions. To include material orientation effects the ε_{in} is then replaced by γ_{in}^{sl}, which is the resolved shear strain on the slip system having the highest Schmid factor, as determined by

$$\frac{\gamma}{2} = n \cdot \varepsilon \cdot s \tag{17}$$

where n is the unit normal to the slip plane and s is the unit normal in the direction of slip. Microstructural evolution is accounted for by including microstructural coarsening kinetics is described by:

$$\Delta r = r_t - r_0 = k(T)t^{1/3} \tag{18}$$

where r_t is the particle diameter at time t, r_0 the initial particle diameter, k(T) is the temperature dependant coarsening rate coefficient and t is time [14, 15]. As the microstructure coarsens the effective slip band spacing increases. Applying this logic to equation 13 yields the relationship in Equation 19,

$$C^* = A\left(\Delta\gamma_{in}^{sl}\right)^{-S}\left(\frac{r_0 + k \cdot t^{1/3}}{r_0}\right) \tag{19}$$

The final physics-based life estimation equation is then provided

$$N_i = \frac{N_S A}{D_0^n}\left(\frac{1}{\Delta\gamma_{in}^{sl}}\right)^s \left\{\exp\left(\frac{Q'}{R \cdot T_{eff}}\right)\frac{\nu}{\nu \cdot t_h + 1/2}\right\}^n \left[\frac{r_0 + k \cdot t^{1/3}}{r_0}\right] \tag{20}$$

By combining parameters one comes to a more user-friendly version of the model,

$$N_i = A_1^n\left(\frac{1}{\Delta\gamma_{in}^{sl}}\right)^s \left\{\exp\left(\frac{Q'}{R \cdot T_{eff}}\right)\frac{\nu}{\nu \cdot t_h + 1/2}\right\}^n \left[\frac{r_0 + k \cdot t^{1/3}}{r_0}\right] \tag{21}$$

where A_1 is a combined parameter which accounts for material lattice vibration (a function of overall energy in the system) among other things. In order to determine the effective activation energy as well as the exponent on the frequency term, two waveforms having different effective temperatures and frequencies were required. Thus the bithermal fatigue (BiF) data presented at the bottom of Table 1 was used in conjunction with TMF data. For a concise discussion on BiF and its waveform, interested readers are directed to reference [16]. The entire experimental data set in Table 1 was used to calibrate the proposed physics-based model.

Using appropriate coarsening rate coefficients (k) from [17] and r_0 = 300nm from [18], the model calibration yielded Q'=95 kJ/mol, n=2.0 and s=2.7. It became apparent during calibration that the lumped parameter A_1 is a function of the mechanical energy imparted to the material via the inelastic shear strain range term ($\Delta\gamma_{in}$). The relationship for A_1 follows:

$$A_1 = 1.2E-6\left(\Delta\gamma_{in}^{sl}\right)^{0.722} \tag{23}$$

The γ_{in}^{sl} term was calculated using Equation 17 with the normal strain replaced with the measured width of test hysteresis loops ($\Delta\varepsilon_{in}$). The results of the model calibration are provided in Figure 7. The physics-based model, as proposed, accurately predicts life for both Bithermal fatigue and Thermomechanical fatigue tests with over 50% of the life estimation falling within a factor of 2.

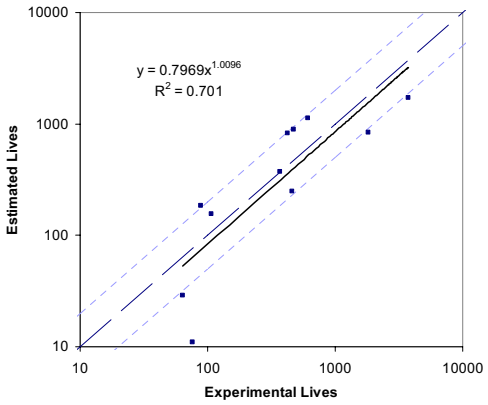

Fig. 7. Physics-based model calibration results

5. Discussion

The results of a multiphased approach to life prediction have been presented. In phase I the Neu-Sehitoglu (N-S) model implementation indicated that the model parameters are somewhat material insensitive. It was also determined that the environmental fatigue module is primarily responsible for N-S model OP TMF life predictions. Results from phase II indicate that the diffusion activation energies, $Q_{\gamma'}$ and Q_{ox}, as well as the strain exponents, α and β, are the critical parameters for N-S life estimation. Once calibrated, the N-S model performs quite well, requiring minimal up-front tests to calibrate, and is very simple to implement. Phase III introduced a physics-based life estimation model which accounts for fatigue, environmental effects, coarsening and test frequency. Though the calibrated model shows promise as a life predictive scheme, the model's intricacy required the use of all available test data to calibrate. As such more TMF and BiF test data is required to test the models efficacy.

Acknowledgements

This work was supported by Pratt & Whitney, East Hartford, CT. We would like to recognize fellow MPRL researcher Patxi Fernandez-Zelaia for his invaluable aid in developing minimization algorithms.

References

[1] Erickson, G.L. Ni-Based Superalloy Developments. 1993. Warrendale, PA, USA: Publ by Minerals, *Metals & Materials Soc* (TMS).

[2] Pineau, A., Antolovich, S. D., High temperature fatigue of nickel-base superalloys - A review with special emphasis on deformation modes and oxidation. *Engineering Failure Analysis.* **In Press, Corrected Proof**.

[3] Oesterle, W., Bettge, D., Fedelich, B., Klingelhoeffer, H., Modelling the Orientation and Direction Dependence of the Critical Resolved Shear Stress of Nickel-Base Superalloy Single Crystals. *Acta Materialia, 2000.* **48**(3): pp. 689-700.

[4] Arakere, N.K. and E. Orozco, Analysis of Low Cycle Fatigue Properties of Single Crystal Nickel-Base Turbine Blade Superalloys. H*igh Temperature Materials and Processes,* 2001. **20**(5-6): pp. 403-419.

[5] Okazaki, M., Sakaguchi, M., Thermo-Mechanical Fatigue Failure of a Single Crystal Ni-Based Superalloy. *International Journal of Fatigue,* 2008. **30**(2): pp. 318-323.

[6] Neu, R.W. and H. Sehitoglu, Thermomechanical fatigue, oxidation, and creep. Part II. Life prediction. *Metallurgical transactions. A, Physical metallurgy and materials science, 1989.* ***20 A****(9): pp. 1769-1783.*

[7] Sehitoglu, H. and D.A. Boismier, Thermo-mechanical fatigue of Mar-M247. Part 2. Life prediction. *Journal of Engineering Materials and Technology, Transactions of the ASME*, 1990. **112**(1): pp. 80-89.

[8] Miller, M.P., D.L. McDowell, and R.L.T. Oehmke, A Creep-Fatigue-Oxidation Microcrack Propagation Model for Thermomechanical Fatigue. J*ournal of Engineering Materials and Technology,* 1992. **114**(3): pp. 282-288.

[9] Gordon, A.P., Crack Initiation Modeling of a Directionally-Solidified Ni-base Superalloy, in *Mechanical Engineering.* 2006, Georgia Institute of Technology: Atlanta, Ga.

[10] Kupkovits, R., Thermomechanical Fatigue Behavior of the Directionally-Solidified Nickel-Base Superalloy CM247LC, in *Mechanical Engineering.* 2009, Georgia Institute of Technology: Atlanta, Ga.

[11] Arakere, N.K., High-temperature fatigue properties of single crystal superalloys in air and hydrogen. *Journal of Engineering for Gas Turbines and Power*, 2004. **126**(3): pp. 590-603.

[12] Diederich, D., Lerch, B., Antolovich, S.D., Observations of Low Cycle Fatigue and Fatigue Crack Propagation Substructures in Waspaloy, in *8th Inter-American Conference on Materials Technology*. 1985: San Juan, Puerto Rico. pp. 7.1-7.6.

[13] McDowell, D.L., Antolovich, S. D., Oehmke, R. L. T., Mechanistic considerations for TMF life prediction of nickel-base superalloys. *Nuclear Engineering and Design*, 1992. **133**(3): pp. 383-399.

[14] Wagner, C., Theory of Precipitate Change by Redissolution (Ostwald Ripening). *Z. Elektrochem*, 1961. **65**: pp. 581-591.

[15] Lifshitz, I.M. and V.V. Slyozov, The kinetics of precipitation from supersaturated solid solutions. *Journal of Physics and Chemistry of Solids*, 1961. **19**(1-2): pp. 35-50.

[16] Gayda, J., Gabb, T., P., Miner, R., V., Halford, G., R.,, Bithermal Low-Cycle Fatigue Behavior of a NiCoCrAlY-Coated Single Crystal Superalloy. 1987, *NASA Technical Memorandum* 89831: NASA Glenn Ressearch Center. pp. 25.

[17] Li, X., N. Saunders, and A.P. Miodownik, The coarsening kinetics of particles in nickel-based alloys. *Metallurgical and Materials Transactions A*: Physical Metallurgy and Materials Science, 2002. **33**(11): pp. 3367-3374.

[18] Cetel, A.D., Duhl, D.N., Second Generation Nickel-Base Single Crystal Superalloy. *Superalloys,* 1988.